Production of slow protonium in vacuum

**N. Zurlo · M. Amoretti · C. Amsler · G. Bonomi ·
C. Carraro · C. L. Cesar · M. Charlton · M. Doser ·
A. Fontana · R. Funakoshi · P. Genova · R. S. Hayano ·
L. V. Jørgensen · A. Kellerbauer · V. Lagomarsino ·
R. Landua · E. Lodi Rizzini · M. Macrì · N. Madsen ·
G. Manuzio · D. Mitchard · P. Montagna ·
L. G. Posada · H. Pruys · C. Regenfus · A. Rotondi ·
G. Testera · D. P. Van der Werf · A. Variola ·
L. Venturelli · Y. Yamazaki**

N. Zurlo (✉) · E. Lodi Rizzini · L. Venturelli
Dipartimento di Chimica e Fisica per l'Ingegneria e per i Materiali, Università di Brescia,
25133 Brescia, Italy
e-mail: zurlo@bs.infn.it

N. Zurlo · E. Lodi Rizzini · L. Venturelli
Istituto Nazionale di Fisica Nucleare, Gruppo Collegato di Brescia, 25133 Brescia, Italy

M. Amoretti · C. Carraro · V. Lagomarsino · M. Macrì · G. Manuzio · G. Testera · A. Variola
Istituto Nazionale di Fisica Nucleare, Sezione di Genova, 16146 Genova, Italy

C. Amsler · H. Pruys · C. Regenfus
Physik-Institut, Zürich University, 8057 Zürich, Switzerland

G. Bonomi
Dipartimento di Ingegneria Meccanica, Università di Brescia, 25123 Brescia, Italy

G. Bonomi · A. Fontana · P. Genova · P. Montagna · A. Rotondi
Istituto Nazionale di Fisica Nucleare, Sezione di Pavia, 27100 Pavia, Italy

C. Carraro · V. Lagomarsino · G. Manuzio
Dipartimento di Fisica, Università di Genova, 16146 Genova, Italy

C. L. Cesar
Instituto de Fisica, Universidade Federal do Rio de Janeiro, Rio de Janeiro 21945-970, Brazil

M. Charlton · D. Mitchard · L. V. Jørgensen · N. Madsen · D. P. Van der Werf
Department of Physics, University of Wales Swansea, Swansea SA2 8PP, UK

M. Doser · A. Kellerbauer · R. Landua
Physics Department, CERN, 1211 Geneva 23, Switzerland

Abstract We describe how protonium, the quasi-stable antiproton-proton bound system, has been synthesized following the interaction of antiprotons with the molecular ion H_2^+ in a nested Penning trap environment. From a careful analysis of the spatial distributions of antiproton annihilation events in the ATHENA experiment, evidence is presented for protonium production with sub-eV kinetic energies in states around $n = 70$, with low angular momenta. This work provides a new two-body system for studies using laser spectroscopic techniques.

1 Introduction

The availability of a high-quality low energy antiproton ($\bar{p}$) beam delivered by the CERN Antiproton Decelerator (AD) to the ATHENA, ATRAP and ASACUSA experiments has permitted the routine production of stable pure antimatter systems (antihydrogen, $\bar{H}$) [1, 2] and metastable mixed matter–antimatter systems (antiprotonic helium or $\bar{p}He^+$) [3, 4], both very important steps towards the goal of testing CPT symmetry in the QED field.

Another metastable exotic atom that is also of great interest is antiprotonic hydrogen ($\bar{p}p$), also called protonium (Pn). Its level structure is similar to that of hydrogen, but binding energies are much larger and its simple two-body nature allows an independent CPT test. In fact, spectroscopic measurements on Pn, made in near-vacuum conditions with high-precision laser techniques, would make it possible to improve the precision of the "(anti)protonic Rydberg" constant or, equivalently, the (anti)proton to electron mass ratio.

Even though Pn has been studied in the past (see e.g. [5, 6]), in this paper we report a radically new method to produce Pn resulting in emission with very low kinetic energy (from some meV to ~ 1 eV) in vacuum conditions that could open the way to laser spectroscopic studies. Previous experiments produced Pn by injecting antiprotons into a molecular hydrogen target (H_2), either liquid or gaseous. This

A. Fontana · P. Genova · P. Montagna · A. Rotondi
Dipartimento di Fisica Nucleare e Teorica, Università di Pavia, 27100 Pavia, Italy

R. Funakoshi · R. S. Hayano · L. G. Posada
Department of Physics, University of Tokyo, Tokyo 113-0033, Japan

Y. Yamazaki
Atomic Physics Laboratory, RIKEN, Saitama 351-0198, Japan

Present Address:
A. Kellerbauer
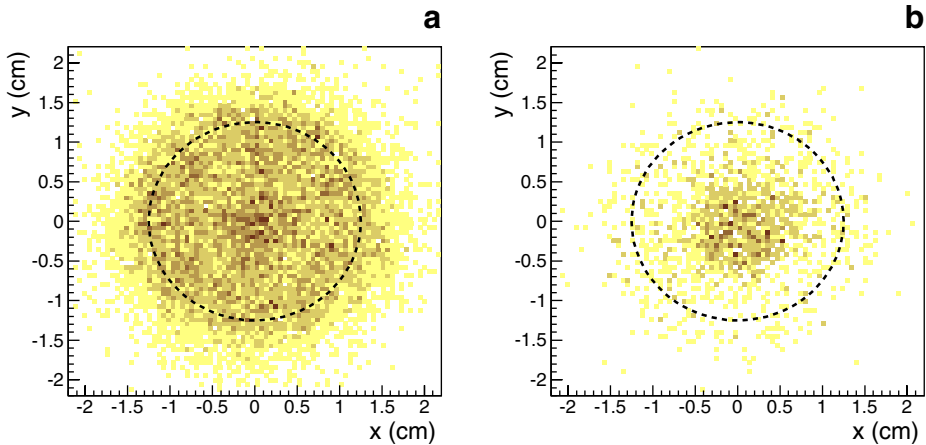Max Planck Institute for Nuclear Research, P.O. Box 103980, 69029 Heidelberg, Germany

Fig. 1 Scatter plot of annihilation vertices projected on a plane perpendicular to the trap axis for **a** cold mixing, **b** hot mixing. The *dashed line* represents the trap wall

results in a Pn lifetime which depends strongly upon the target density due to the effect of collisional de-excitation and which makes spectroscopy impossible. In the ATHENA apparatus Pn has been produced after a "chemical" reaction between $\bar{p}$'s and molecular hydrogen ions (H_2^+) trapped together with positrons (e^+) in a nested Penning trap. Protonium production accompanies the $\bar{H}$ production described in [1], and here we describe how the two modes of $\bar{p}$ annihilation have been distinguished (see also [7]).

2 Experimental details

The ATHENA apparatus, described extensively in [8], consisted of a multi-electrode system of cylindrical Penning traps, 2.5 cm in diameter and ∼1 m in length kept in an axial magnetic field of 3 T. In the 15 K cryogenic environment of the trap, only hydrogen and helium were present in gaseous form, giving a residual pressure of ∼ 10^{-12} Torr. Antiprotons from the AD were caught, cooled by electrons and stored in the so-called mixing trap. The latter is a nested Penning trap, approximately 10 cm long, that allowed e^+s and $\bar{p}$'s to be confined simultaneously. Under typical conditions the trap contained a spheroidal plasma of ∼ 3.5×10^7 e^+ and ∼ 10^4 $\bar{p}$'s. The resulting $\bar{p}$ annihilations were monitored for ∼ 60 s by detectors [9] that, recording the passage of the charged pions, allowed reconstruction of annihilation vertices with an uncertainty of a few mm.

In typical operating conditions, annihilation of $\bar{p}$'s originate from:

– $\bar{H}$ formation followed by annihilation on the electrode surface [1, 10];
– $\bar{p}$ annihilation in some well-defined "spots" on the electrode walls due to radial transport [11];
– annihilation following interactions with residual gas atoms or ions present in the trap.
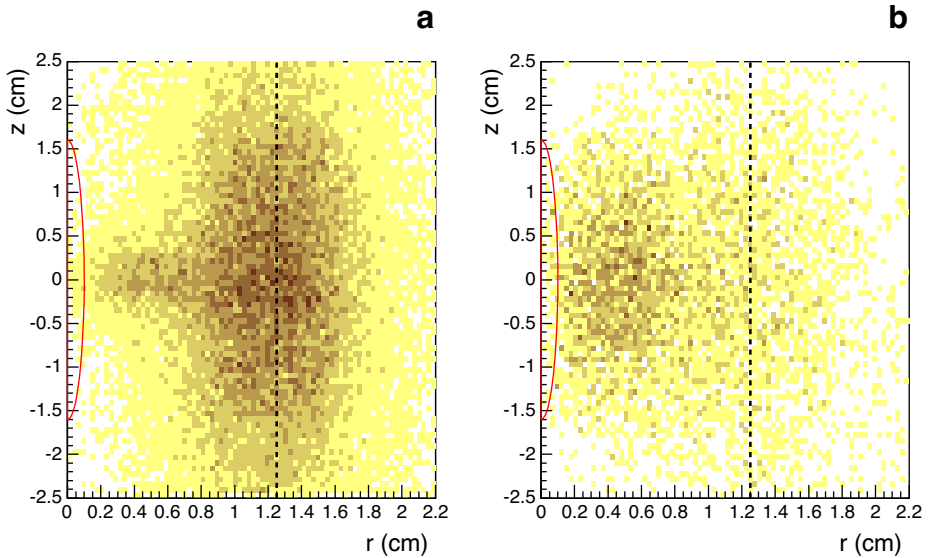
Fig. 2 Scatter plot of annihilation vertices as a function of *r* and *z* for **a** cold mixing, **b** hot mixing. The *dashed line* represents the trap wall. The *semi-ellipse* indicates the size and position of the positron cloud

It was shown in [12] that, when the e^+ cloud was kept at the trap environment cryogenic temperature of ~ 15 K (a situation called "cold mixing" hereafter), annihilations were mainly due to H̄, even if some annihilations near the trap axis were present (see also Fig. 1a). On the contrary, when the e^+ cloud was heated (by a radio-frequency drive applied to an electrode of the trap [13, 14]) to a temperature, T_e, of several thousand K (about 8,000 K for the data reported here, which we call "hot mixing" hereafter) H̄ formation was strongly suppressed [15] and $\bar{p}$s annihilated mainly without forming H̄ (see also Fig. 1b).

In the following, we will study in detail the latter annihilations.

3 Results and discussion

In Fig. 1, we report the *x–y* scatter plots (both coordinates are in the plane perpendicular to the trap axis) for cold and hot mixing data. In Fig. 2, the corresponding *r–z* scatter plots are reported (where $r = \sqrt{x^2 + y^2}$ is the radial position, i.e. the distance from the trap axis, and *z* is the axial coordinate, measured from the symmetry plane of the trap).

Even though all the distributions are broadened by the uncertainty in the vertex reconstruction, it is clear that two different structures are merged in the cold mixing case, while in hot mixing just one appears. For cold mixing, besides the annihilations on the trap wall situated at $r = 1.25$ cm due mainly to H̄ (as shown in [12]) and having a relatively wider *z*-distribution [10], there are some annihilations situated at smaller *r* and with a very sharp *z*-distribution (see also Fig. 5b). For hot mixing only the latter are present, though their axial distribution is broader, as is the radial distribution (see also Fig. 4a,b).
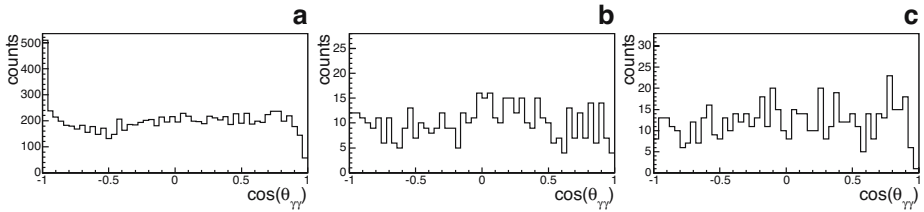
Fig. 3 Histogram of the cosine of the angle between the two detected photons ($\cos(\theta_{\gamma\gamma})$, see text) for **a** cold mixing, on the wall ($r > 1$ cm); **b** cold mixing, near the trap axis ($r < 0.5$ cm); **c** hot mixing

The capability of the ATHENA detector to detect the spatial and temporal coincidence between $\bar{p}$ and e^+ annihilations, and therefore to separate $\bar{H}$ from other annihilations, allows us to infer that for hot mixing almost all annihilations (even near the wall) are not due to $\bar{H}$, while for cold mixing we have to distinguish between annihilations near the trap axis, that are not due to $\bar{H}$ (apart from a few poorly reconstructed vertices), and near the wall, where the number of non-$\bar{H}$ annihilations is negligible.

This is clear if we look at Fig. 3, where we consider annihilations happening in coincidence with two (and only two) photons detected, and we plot the cosine of the angle between the two detected photons, $\cos(\theta_{\gamma\gamma})$. This distribution should have a peak in $\cos(\theta_{\gamma\gamma}) = -1$ if annihilations are due to $\bar{H}$, because of the two back-to-back 511 keV photons produced by the e^+ annihilation, while we do not expect any peaks for annihilations not related to $\bar{H}$. The former is the case for cold mixing on the wall (Fig. 3a), whilst the latter is the case for cold mixing near the trap axis (Fig. 3b) and for hot mixing (Fig. 3c).

It is notable that the axial extent of the annihilation distributions is small compared with the size of the nested trap, so they cannot be in-flight annihilations of $\bar{p}$'s on residual gas. However, their radial extent is too large to be explained by in-flight annihilations on positive ions trapped inside the positron well. So, only a process involving $\bar{p}$ interaction with an ion to form a neutral system that can annihilate in flight, perhaps after leaving the positron well in the central part of the trap, can explain the data.

Time-of-flight measurements following charged particle ejection from the trap excluded the presence of protons and of ions of atoms more massive than helium. However, reactions of $\bar{p}$ with helium ions would give distributions that do not match the data, since $\bar{p}\,He^{++}$ gives rise to a charged system followed by rapid annihilation, and also for $\bar{p}\,He^+$ the residual electron would be ejected in less than 10 ns [16], again giving rise to a charged system.

Further important information on the $\bar{p}$-system formed can be found by exploiting the number of tracks from each annihilation vertex, corresponding to the number of charged pions produced during the annihilation, since this depends on the particle with which the $\bar{p}$ annihilates (see e.g. [17]). Table 1 shows the ratios, R_{23}, of the number of the reconstructed annihilation vertices having two tracks to those with three tracks, for different data samples. In order to have a better understanding of these data, a Monte Carlo simulation of $\bar{p}p$ (i.e. Pn) annihilations inside the ATHENA apparatus has been performed using the GEANT3 program. Comparing these data, we see that annihilations on wall differ from those originating inside the trap, which are compatible with $\bar{p}p$ annihilations both for cold mixing and hot mixing.

Table 1 Experimental and Monte Carlo results for the number of charged pion tracks due to $\bar{p}$ annihilations

Data set	Ratio R_{23} on wall	Ratio R_{23} at centre
Cold mixing	1.35±0.01	1.22±0.04
Hot mixing	1.38±0.10	1.17±0.04
$\bar{p}$s only (no mixing)	1.40±0.03	
Monte Carlo $\bar{p}p$	1.19±0.01	

Combining this information, we infer that the most probable $\bar{p}$–ion reaction is:

$$\bar{p} + H_2^+ \rightarrow Pn(n, l) + H. \tag{1}$$

where the Pn leaves the central part of the trap (because it is neutral), and has an exponentially distributed annihilation lifetime (depending on n and l). For relatively high n, Pn is formed in a metastable state and its lifetime can be greater than $1 \mu s$ [18].

The H_2^+ ions required for reaction (1) may have been created during the positron loading procedure [19], due to collisions with the residual H_2 gas, or during $\bar{p}$ loading (similarly to that reported in [20]). Measurements of charge during the dump of the trapped particles has indicated that the number of ions could be as high as 10^5, depending on the vacuum conditions.

In order to check our hypothesis, we performed a self-standing Monte Carlo simulation to reproduce the observed annihilation distributions for hot mixing and cold mixing in the following way:

– We used the information we have on the e^+ plasma shape [13, 14] to generate the Pn starting point distributions (in particular, it was found that the e^+ plasma was approximately a spheroid with radius r_p=1 mm and axial half-length z_p=16 mm, rotating with a frequency of 300 kHz; i.e. a surface velocity of about 2,000 ms^{-1}).
– Assuming that Pn is produced in thermal equilibrium with the e^+ plasma, and knowing that Pn must inherit the drift velocity from its charged components, we generated a velocity distribution summing the thermal Maxwellian isotropic velocity (with a mean value fixed by the measured temperature of the e^+ plasma) with a velocity along the tangential direction (that is the same as inferred by the measured parameters of the e^+ plasma, since the drift doesn't depend on either the mass or the charge of the particle).

Starting with hot mixing (8,000 K), the simulation was performed assuming that the Pn was produced on the surface of the e^+ spheroid (characterized by the parameters above), with a Gaussian distribution along z (having $\sigma = 10$ mm and being limited to $|z| < z_p$) or alternatively inside the e^+ spheroid with a uniform density. The result is nearly independent of the assumed distribution of starting positions, since the system is dominated by the thermal velocity of 5,600 ms^{-1}. The simulated radial and axial distributions for the best fitted mean lifetime (1.1 μs) are superimposed on the experimental data in Fig. 4. The agreement is good, and in particular the simulation shows that about 25% of the Pn produced reaches the wall, as observed, and it also predicts that the axial distribution near the wall is slightly wider than that near the axis (Fig. 4b,c) due to the essentially isotropic spreading.
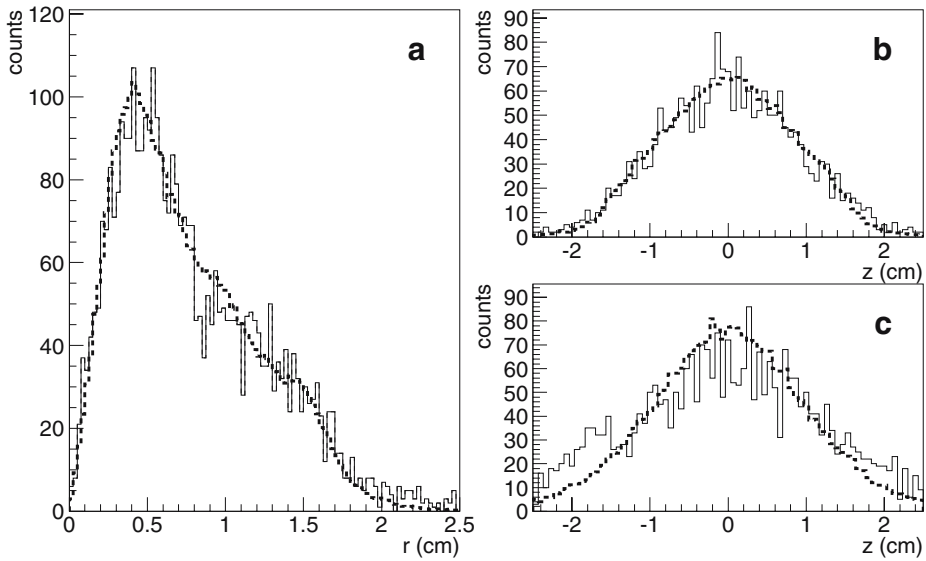
Fig. 4 Distributions of annihilation vertices for hot mixing (*continuous line*), with superimposed Monte Carlo simulation results (*dashed line*). **a** radial distribution; **b** axial distribution, for events near the trap axis ($r < 0.5$ cm); **c** axial distribution, for events near the trap wall ($r > 1$ cm)

For cold mixing the analysis is less straightforward, because the $\bar{\text{H}}$ contribution on the trap wall must be subtracted. To do so, we considered the difference between a radial distribution taken in a z-slice where Pn is present (e.g. $|z| < 0.5$), and one where there is no Pn (e.g. 0.5 cm $< |z| < 1.5$ cm), normalized on the tail for $r > 1.5$ cm, which is essentially $\bar{\text{H}}$ only. The result is shown in Fig. 5a. For the axial distribution, isolating the Pn signal is much simpler, because only annihilations near the axis of the trap need be considered (Fig. 5b).

In order to simulate the cold mixing distributions, the parameters (r_p, z_p, frequency rotation) of the e^+ plasma were the same as for hot mixing, and we generated Pn with a thermal velocity corresponding to 15 K (250 ms^{-1} along each direction). However, in this case it is necessary to assume that Pn is produced in a very narrow region around $r = r_p$ and $z = 0$ (we generated it with a Gaussian distribution along z with $\sigma = 2.5$ mm). The best fitted mean lifetime is 1.1 μs, as found for hot mixing.

The agreement between the experimental and Monte Carlo data is good (Fig. 5a,b). Furthermore, Monte Carlo results show that less than 0.5% of Pn reached the wall in this case, thus confirming the consistency of our normalization technique.

For cold mixing, we were also able to analyze another data sample, where the positron plasma had different parameters (r_p=2.5 mm, z_p=18 mm, rotation frequency of 80 kHz, surface velocity of about 1,300 ms^{-1}). Following the same prescription, we have reproduced the radial distribution of this sample (Fig. 5c), showing there is a notable difference between the distribution of Pn annihilations in this case and that for a narrower e^+ plasma.

It has to be stressed that it is impossible to reproduce the experimental results unless Pn is produced in a narrow region straddling the "equator" of the e^+ spheroid. A possible and quite straightforward way to explain this, is to assume that there is
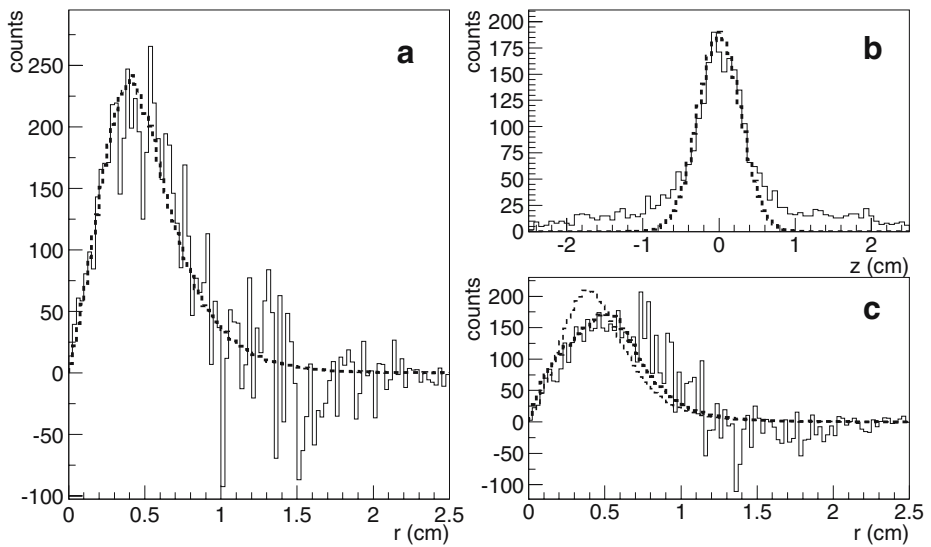
Fig. 5 Distributions of annihilation vertices for cold mixing, (*continuous line*), with superimposed Monte Carlo simulation results (*dashed line*). **a** radial distribution, after removing the H̄ contribution as discussed in the text; **b** axial distribution, for events near the trap axis ($r < 0.5$ cm); **c** radial distribution, for the cold mixing sample with wider positron plasma (in this case, the *thick dashed line* corresponds to Monte Carlo results with the correct plasma parameters, while the *thin dashed line* corresponds to Monte Carlo results with the parameters of the narrower positron plasma; see text)

some kind of (partial) separation between the e^+ and the H_2^+ ions, as expected in case of thermal equilibrium (see [21, 22]), and as has been observed for a mixture of e^+ and $^9Be^+$ in [23, 24]. In fact, for our experimental conditions, assuming thermal equilibrium, H_2^+ ions experience a centrifugal potential barrier of the order of 10 meV meaning that, for 15 K, their thermal energy (~ 1 meV) is not enough to allow the ions to penetrate the e^+ plasma. However, for 8,000 K, the barrier is negligible compared to the thermal energy (~ 700 meV) of the ions such that they will be distributed uniformly inside the plasma.

Another constraint from our Monte Carlo simulation relates to the Pn kinetic energy. In fact, the hot mixing and the cold mixing data cannot be reproduced using the same mean lifetime for both of them if the system has a recoil kinetic energy of the order of 1 eV or greater. This probably means that the $\bar{p}$-H_2^+ collision happens preferentially as a resonant transfer, i.e. the dissociation energy of H_2^+ is taken care of by the binding energy of Pn, so that its energy level, n, should be around 70.

Because we find a mean lifetime of about 1.1 μs, it can be inferred [18] that the orbital angular momentum, l, should be around 10. This could be a consequence of the fact that, with such a slow relative collisional velocity, the H_2^+ molecular ion will be strongly polarized, giving rise to an almost collinear collision.

4 Conclusions

In this paper, we have presented evidence for the production of protonium in vacuum. It is formed in a metastable state (with a lifetime of about 1.1 μs, independent

of the environment temperature) and with near-thermal kinetic energies (varying from some meV to less than 1 eV). The number of produced protonium atoms was about 100 for each mixing cycle (~ 100 s), in which around 10^4 $\bar{p}$s were injected into the mixing trap, while the estimated number of ions trapped with the positrons was typically $10^4 - 10^5$. Taking into account the recently achieved capability of accumulating $\sim 10^8$ H_2^+ and storing $\sim 5 \times 10^6$ $\bar{p}$s in some minutes [25, 26], our result opens up the possibility of performing detailed spectroscopic measurements on protonium as a probe of fundamental constants and symmetries.

References

 1. Amoretti, M., et al.: Nature **419**, 456 (2002)
 2. Gabrielse, G., et al.: Phys. Rev. Lett. **89**, 213401 (2002)
 3. Yamazaki, T., et al.: Phys. Rep. **366**, 183 (2002)
 4. Hori, M., et al.: Phys. Rev. Lett. **96**, 243401 (2006)
 5. Batty, C.J.: Rept. Prog. Phys. **52**, 1165 (1989)
 6. Montanet, L.: Nucl. Phys. A **692**, 383c (2001)
 7. Zurlo, N., et al.: Phys. Rev. Lett. **97**, 153410 (2006)
 8. Amoretti, M., et al.: Nucl. Instrum. Methods A **518**, 679 (2004)
 9. Regenfus, C.: Nucl. Instrum. Methods A **501**, 65 (2003)
10. Madsen, N., et al.: Phys. Rev. Lett. **94**, 033403 (2005)
11. Fujiwara, M.C., et al.: Phys. Rev. Lett. **92**, 065005 (2004)
12. Amoretti, M., et al.: Phys. Lett. B **578**, 23 (2004)
13. Amoretti, M., et al.: Phys. Rev. Lett. **91**, 055001 (2003)
14. Amoretti, M., et al.: Phys. Plasmas **10**, 3056 (2003)
15. Amoretti, M., et al.: Phys. Lett. B **583**, 59 (2004)
16. Korobov, V.I.: Phys. Rev. A **67**, 062501 (2003)
17. Balestra, F., et al.: Nucl. Phys. A **491**, 541 (1989)
18. Hayano, R.S.: Nucl. Phys. A **655**, 318c (1999)
19. Jørgensen, L.V., et al.: Phys. Rev. Lett. **95** 025002 (2005)
20. Gabrielse, G., et al.: Phys. Lett. B **455**, 311 (1999)
21. Dubin, D.H.E., O'Neil, T.M.: Rev. Mod. Phys. **71**, 87 (1999)
22. O'Neil, T.M.: Phys. Fluids **24**, 1447 (1981)
23. Jelenković, B.M., et al.: Phys. Rev. A **67** 063406 (2003)
24. Jelenković, B.M., et al.: Nucl. Instrum. Methods B **192** 117 (2002)
25. Kuroda, N., et al.: Phys. Rev. Lett. **94**, 023401 (2005)
26. Oshima, N., et al.: Phys. Rev. Lett. **93**, 195001 (2004)